Science of the Total Environment 751 (2021) 141628

Contents lists available at ScienceDirect

Science of the Total Environment

journal homepage: www.elsevier.com/locate/scitotenv

Heterotrophic bacterioplankton responses in coral- and algae-dominated Red Sea reefs show they might benefit from future regime shift

Luis Silva [a,*], Maria Ll. Calleja [a,b], Snjezana Ivetic, Tamara Huete-Stauffer [a], Florian Roth [a,c,d], Susana Carvalho [a], Xosé Anxelu G. Morán [a]

[a] King Abdullah University of Science and Technology (KAUST), Red Sea Research Center, Thuwal 23955-6900, Saudi Arabia
[b] Department of Climate Geochemistry, Max Planck Institute for Chemistry (MPIC), Hahn-Meitner-Weg 1, 55128 Mainz, Germany
[c] Baltic Sea Centre, Stockholm University, 11418 Stockholm, Sweden
[d] Tvärminne Zoological Station, University of Helsinki, 00100 Helsinki, Finland

HIGHLIGHTS

- Heterotrophic bacteria responses to coral- and algal-DOM changed seasonally.
- DOC concentrations from both communities peaked during the warmer months.
- Warmer months led to higher bacterial growth rates in algal-DOM.
- Algal-DOM was processed more efficiently during the warmer months.

GRAPHICAL ABSTRACT

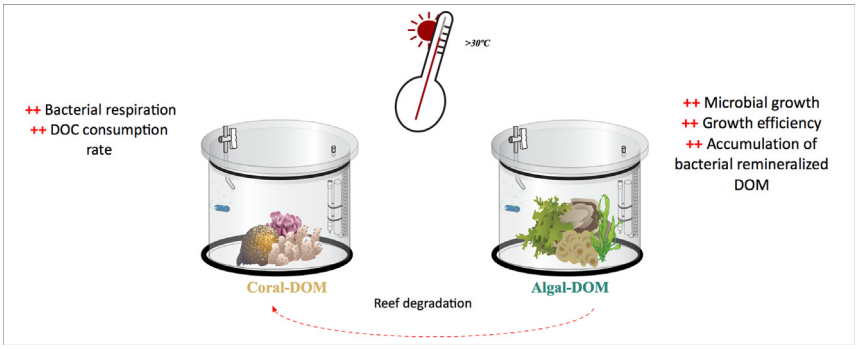

ARTICLE INFO

Article history:
Received 20 April 2020
Received in revised form 6 August 2020
Accepted 9 August 2020
Available online 16 August 2020

Editor: Henner Hollert

Keywords:
Coral-algae shifts
DOM lability
Heterotrophic bacteria
Growth rates
Bacterial growth efficiencies
Activation energies

ABSTRACT

In coral reefs, dissolved organic matter (DOM) cycling is a critical process for sustaining ecosystem functioning. However, global and local stressors have caused persistent shifts from coral- to algae-dominated benthic communities. The influence of such phase shifts on DOM nature and its utilization by heterotrophic bacterioplankton remains poorly studied. Every second month for one year, we retrieved seawater samples enriched in DOM produced by coral- and algae-dominated benthic communities in a central Red Sea reef during a full annual cycle. Seawater incubations were conducted in the laboratory under in situ temperature and light conditions by inoculating enriched DOM samples with bacterial assemblages collected in the surrounding waters. Dissolved organic carbon (DOC) concentrations were higher in the warmer months (May–September) in both communities, resulting in higher specific growth rates and bacterial growth efficiencies (BGE). However, these high summer values were significantly enhanced in algal-DOM relative to coral-DOM, suggesting the potential for bacterioplankton biomass increase in reefs with algae replacing healthy coral cover under warmer conditions. The potential exacerbation of heterotrophic bacterial activity in the ongoing widespread regime shift from coral- to algae-dominated communities may have detrimental consequences for the overall health of tropical coral reefs.

* Corresponding author.
E-mail address: luis.ribeirodasilva@kaust.edu.sa (L. Silva).

https://doi.org/10.1016/j.scitotenv.2020.141628

1. Introduction

Coral reefs are considered one of the most productive and biodiverse ecosystems on Earth, even though they are found in the largely oligotrophic waters of the tropics (Atkinson et al., 2003; Done et al., 1996; McDole Somera et al., 2016). The high productivity of coral reefs is mainly attributed to the efficient cycling of organic matter and nutrients (Done et al., 1996; Haas et al., 2016). In coral reef ecosystems, dissolved organic carbon (DOC) is mainly released by benthic primary producers, such as reef algae and scleractinian corals (Haas et al., 2010; Naumann et al., 2010; Wild et al., 2011). By taking up DOC, heterotrophic bacteria contributes significantly to ecosystem metabolism as the assimilated DOC can either be remineralized and released as carbon dioxide (bacterial respiration) or assimilated into new biomass (bacterial production) and available for higher trophic levels (Azam et al., 1983; Azam and Malfatti, 2007; Cotner and Biddanda, 2002; Kirchman et al., 2009). Understanding how the balance between these two metabolic pathways is controlled is crucial towards the determination of the ecological role of bacteria in aquatic systems and their impact on biogeochemical cycles (Alonso-Sáez et al., 2008; del Giorgio and Cole, 1998; Robinson, 2008). A useful variable relating bacterial production and respiration is bacterial growth efficiency (BGE), representing the proportion of assimilated carbon that is converted into biomass and ultimately might be processed by other members of the marine food web.

In the past decades, climatic and pervasive local stressors have caused rapid declines in live coral cover with persistent shifts to communities with a predominance of filamentous turf- and macroalgae (Bellwood et al., 2004; Done, 1992; Hughes et al., 2018; Pratchett et al., 2007). The release of higher quantities of bioavailable DOC from algae can fuel the growth of planktonic heterotrophic bacteria (Haas et al., 2011; Nelson et al., 2013), potentially causing localized hypoxia and coral tissue death (Barott et al., 2009, 2012; Smith et al., 2006). Moreover, labile algae-derived DOC can favor the growth of copiotrophic bacteria and increase virulence factors (Cárdenas et al., 2018; Morrow et al., 2011; Nelson et al., 2013), as described by the "Dissolved organic matter, Disease, Algae, Microbes" (DDAM) model (Barott and Rohwer, 2012; Dinsdale and Rohwer, 2011). Ultimately, the shifts in reef benthic communities may influence the entire ecosystem functioning by affecting biogeochemical cycles, especially that of carbon (Haas et al., 2016, 2011; Wild et al., 2011). However, knowledge about the interaction between dissolved organic matter (DOM) and heterotrophic bacterioplankton under these phase shifts is still limited and mostly based on laboratory DOM enrichments from single benthic species. The few studies involving incubations of bacterial assemblages and different DOM exudates are also limited to single time point within the year (Haas et al., 2011, 2013; Nelson et al., 2013; Silveira et al., 2015, 2019), further limiting our capability to extend laboratory findings to natural communities during an annual cycle.

To fill this gap, we evaluated for the first time the seasonal variability of the effect of seawater naturally enriched in DOM from tropical coral- and algae-dominated communities on the growth rates and efficiencies of epipelagic heterotrophic bacterioplankton. Bi-monthly in a central Red Sea reef we applied a novel in situ incubation system (Roth et al., 2019) to prepare seawater cultures (Ammerman et al., 1984) during a full annual cycle (March 2017–January 2018). Through simultaneous monitoring of heterotrophic bacterioplankton total growth and DOC uptake, we were able to determine the different bioavailability of DOC released by natural reef communities dominated by corals and by algae (Ammerman et al., 1984; Lønborg et al., 2016b, 2018). We additionally assessed the physiological structure (sensu del Giorgio and Cole, 1998) of heterotrophic bacterial communities and complemented the bulk DOM measurements (i.e. DOC and DON concentrations) with a detailed assessment of its fluorescent fraction in order to better evaluate its composition, lability and reactivity (Catalá et al., 2015; Coble et al., 2014). Recent experiments have shown that the nature of DOM released by algae and corals differs substantially (e.g. Haas and Wild, 2010; Mueller et al., 2014; Quinlan et al., 2018; Wild et al., 2010), with consequences for the growth and standing stocks of heterotrophic bacteria (Haas et al., 2011; Nelson et al., 2013). Based on the above, we hypothesized that: a) DOM availability and composition differs between the two natural reef communities (i.e., coral- vs. algae-dominated); b) the standing stocks and specific growth rates of heterotrophic bacterioplankton responses will be enhanced by algal DOM and; c) seasonality will influence the observed responses.

2. Material and methods

2.1. Sampling site and experimental design

We performed in situ incubations at Abu Shosha reef located on the west coast of Saudi Arabia (22°18.272′N; 39°2.9617′E), in the central east coast of the Red Sea. The Red Sea is a semi-enclosed marine basin hosting one of the most diverse coral reef systems worldwide (Berumen et al., 2019b). Coral reefs within the Red Sea have been able to cope with higher temperature and saline waters than other tropical places. However, within the last decade they have experienced severe heat episodes threatening coral health (Berumen et al., 2019a; Monroe et al., 2018), and making them more vulnerable to benthic reef algae growth. In situ incubations were performed bi-monthly from March 2017 until January 2018 in Abu Shusha reef sites at a water depth of 4–7 m. The reef is characterized by a heterogeneous mosaic of patches of communities dominated either by corals or by algae, thus allowing the study of both types of communities ("coral-dominated" and "algae-dominated") under identical environmental conditions. The communities where the in situ incubations were performed were carefully chosen to fulfil the following characteristics: i) Coral-dominated communities were defined by having >40% coral cover but <10% algae cover; ii) Algae-dominated communities were defined by having >40% algae cover but <10% coral cover; iii) were surrounded by sand at the semi-exposed side of the reef within a 50 × 50 m area and had to fit into the incubation chambers (max. diameter 50 cm, max. height 39 cm). Although acknowledging that DOM and other metabolites present in each chamber can have multiple sources (e.g. different molecules can be produced by different genera), for logistical reasons we refrained from assigning the relative contribution of species or genera and rather aimed to look at the community as a whole. As the incubation chambers were designed to be coral- and algal-dominated communities, hereafter and for our experiments we will refer to them as coral-DOM and algal-DOM, respectively.

Benthic chambers were made from polymethyl methacrylate cylinders with a gas-tight removable lid. Each chamber was equipped with temperature and dissolved oxygen sensors together with an individual water circulation pump and two sampling ports. In situ incubations were started at 9:00 am after tightly securing the lids and lasted for about 2 h. More detail can be found in Roth et al. (2019) (Fig. 1A, B). At the end of the incubations, we collected 6–8 L of the enclosed water from two chambers of each community type. The water was pumped up to the boat and subsequently filtered using a dual- stage filter cartridge (0.2 and 0.2 μm, Pall, ACROPAK 500 cm^2 Supor Membrane) to separate the DOM from the particulate fraction (Fig. 1A, C). Meanwhile, an inoculum of heterotrophic bacteria was collected using a Niskin bottle from the water column (approximately 5 m) above the benthic chambers and filtered through a PureFlo Capsule filter (0.8 μm, Zen Pure) to remove bacterial grazers. Before using them, both ACROPAK and PureFlo filters were rinsed with MilliQ water, and washed with 4% hydrochloric acid, and subsequently rinsed with MilliQ water. 1 L of water from each chamber was used first to rinse the filters prior to collecting experimental DOM samples. Roth et al. (submitted) showed that 2 h of in situ incubation were enough to significantly enrich background DOM (on average we observed 7.7 and 6.2% overall increase in DOC concentration in coral and algae-dominated communities, respectively). Environmental samples taken before the onset of in situ

incubations in the vicinity of the chambers showed values similar to those measured immediately after enclosing the incubation chambers. After the 2 h incubation period, the additional environmental samples collected showed consistently lower DOC concentrations (on average 10% lower) than the values measured within the different incubation chambers (Supplementary Table S1). Once in the laboratory, the bacterial inoculum was added to the DOM-enriched water using a 1/11 dilution (600–800 mL into 6–8 L). We then performed laboratory incubations for four days using 2 L polycarbonate bottles in duplicates for the DOM-enriched water collected from each in situ chamber sampled, following the seawater culture method (Ammerman et al., 1984). Laboratory incubations were performed in temperature-controlled incubators (Percival – I-22LLVL) with in situ light (12 h light/12 h dark cycle) and temperature conditions. Laboratory incubations were conducted mimicking the in situ diel sunlight cycle, thus aimed at specifically including the potential role of photoheterotrophic bacteria in the carbon fluxes and specific growth rates estimations. Although the role of this functional group of bacteria has been frequently neglected by conducting incubations in continuous darkness (Ruiz-González et al., 2012, 2013), it may be substantial (Arandia-Gorostidi et al., 2020), especially in low latitude oligotrophic environments (Church et al., 2004; Ferrera et al., 2017; Michelou et al., 2007)

Laboratory incubations matched (±0.7 °C) in situ temperatures (Fig. 1D). Subsamples for inorganic nutrients, DOC, fluorescent DOM (FDOM), bacterial abundance and bacterial single–cell physiological properties were collected along the incubation time. Due to the dilution factor applied, samples were collected two or three times per day to better capture the exponential phase of growth within the first two days, and daily during the following days. Laboratory incubations lasted no longer than four days, ending once the stationary or decay phase of bacterioplankton growth was observed.

2.2. Dissolved inorganic nutrients and dissolved organic carbon (DOC) and nitrogen (DON)

Samples for the analysis of inorganic nutrients were filtered through 0.2 μm Millipore® polycarbonate filters and stored frozen at −20 °C until being processed. Analyses of Nitrate (NO_3^-), nitrite (NO_2^-) and phosphate (PO_4^{3-}) were performed in a segmented flow analyzer from Seal Analytical. Limits of quantification were 0.2, 0.06 and 0.01 μmol L^{-1} for NO_3^- NO_2^- and PO_4^{3-} respectively. Acid-washed glassware was used for the preparation of all standards using nutrient-free artificial seawater matrix.

Samples for the analysis of DOC and total dissolved nitrogen (TDN) were filtered through 0.2 μm Millipore® polycarbonate filters. After the filtration, samples were acidified with phosphoric acid down to a pH of 1–2 and kept at 4 °C until further analysis by high temperature catalytic oxidation (HTCO) using a Shimadzu TOC-L. To monitor the accuracy of DOC and TDN concentration measurements, we used reference material of deep-sea carbon (42–45 μmol C L^{-1} and 31–33 μmol N L^{-1}) and low carbon water (1–2 μmol C L^{-1}). DON concentrations were calculated after subtracting the dissolved inorganic nitrogen (DIN) to the TDN (DON = TDN - DIN), where DIN (μmol C L^{-1}) = $[NO_3^-] + [NO_2^-]$.

During the laboratory incubations, we estimated the consumption and production rates of inorganic nutrients, DOC and DON (in μmol L^{-1} d^{-1}) as the difference between the initial and final concentration divided by incubation time during the exponential bacterial growth phase. Positive and negative values were considered as production and consumption, respectively.

2.3. DOM fluorescence measurements

Samples for fluorescent dissolved organic matter (FDOM) analysis were filtered through 0.2 μm Millipore® polycarbonate filters. UV-VIS fluorescence spectroscopy was measured using a HORIBA Jobin Yvon AquaLog spectrofluorometer with a 1 cm path length quartz cuvette. The three-dimensional fluorescence excitation emission matrices (EEMs) were recorded by scanning the excitation range between 240 and 600 nm and emission wavelength range of 250–600 nm, both at 3 nm increments and using an integration time of 8 s. The fluorescence spectra was corrected and calibrated using post-processing steps according to (Murphy et al., 2010). Concisely, Raman-normalized Milli-Q blanks were subtracted to remove the Raman scattering signal (Stedmon et al., 2003). All fluorescence spectra were Raman Area (RA) normalized via the subtraction of daily blanks performed using Ultra-Pure Milli-Q sealed water (Certified Reference, Starna Cells). Inner-filter correction (IFC) was not applied due to the low absorption coefficient of the samples: 2.7 ± 0.5 m^{-1} (average ± s.d.) at 250 nm, that is, much lower than the threshold of 10 m^{-1} above which this correction is required (Stedmon and Bro, 2008). RA normalization, blank subtraction, and generation of EEMs were performed using MATLAB (version R2015b). The EEMs obtained were subjected to PARAFAC modeling using drEEM Toolbox for Matlab (Murphy et al., 2013). Before the analysis, Rayleigh scatter bands were trimmed. A six-component model was validated using split-half validation and random initialization (Stedmon and Bro, 2008): peak C1 at Ex/Em 261/ 450 nm (represents a humic-like peak A (Coble, 2007), peak C2 at Ex/Em 324/ 380 nm (corresponds to humic-like peak M (Coble, 2007), peak C3 at Ex/Em 267/310 (corresponds to protein-like peak B (Coble, 2007) and is attributed to tyrosine), peak C4 at Ex/Em 288/340 nm (corresponds to protein-like peak T (Coble, 2007) and attributed to tryptophane), peak C5 at Ex/Em 261/505 nm (corresponds to un unknown humic-like peak), and peak C6 at Ex/Em 261/350 nm (correspond to unknown protein-like peak that we attributed to contamination and did not consider in further analysis). The maximum fluorescence (Fmax) of each component is reported in Raman units (RU). The fluorescence index (FI) was calculated as the fluorescence intensity ratio at 450 nm and 500 nm emission and 370 nm excitation (McKnight et al., 2001). The humification index (HIX) was obtained as the ratio of peak area under emission spectra between 435 and 480 and 300–345 nm at an excitation wavelength of 254 nm (Ohno, 2002). The biological index (BIX) was obtained as the ratio of emission at 380 and 430 nm at 310 nm of excitation wavelength (Huguet et al., 2009).

2.4. Single-cell physiological groups of heterotrophic bacteria

We measured the abundances of four different single-cell groups of heterotrophic bacteria (Del Giorgio and Gasol, 2008). We followed the methodology detailed in Gasol and Moran (2015). High nucleic acid (HNA) and low nucleic acid (LNA) content cells were distinguished by their green fluorescence signal after being stained with SybrGreen (Marie et al., 1997). Samples were previously fixed with a final concentration of 1% paraformaldehyde and 0.05% glutaraldehyde, deep-frozen in liquid nitrogen, and stored at −80 °C until analysis. Samples were thawed, stained, and run in a BD FACSCanto flow cytometer within 1 to 2 months.

Cyanobacteria, mostly *Synechococcus* (no *Prochlorococcus* was observed), when present, were also easily differentiated by their higher red fluorescence signal due to chlorophyll *a* and orange fluorescence due to phycoerythrin.

The cells with intact membranes (hereafter '*live*') were distinguished from membrane-damaged cells (hereafter '*dead*') by combining two nucleic acid stains, SybrGreen (Molecular Probes) and Propidium Iodide (Sigma Chemical Co.) (Grégori et al., 2001). *Live* and *dead* cells were analyzed without prior fixation within 1 h of collection. Actively respiring cells (CTC+) were also analyzed in vivo after an incubation period of 90 min in the dark with the CTC-tetrazolium salt. They were distinguished by red fluorescence signal that indicates the deposition of oxidized crystals of the CTC-tetrazolium salt (Sherr et al., 1999).

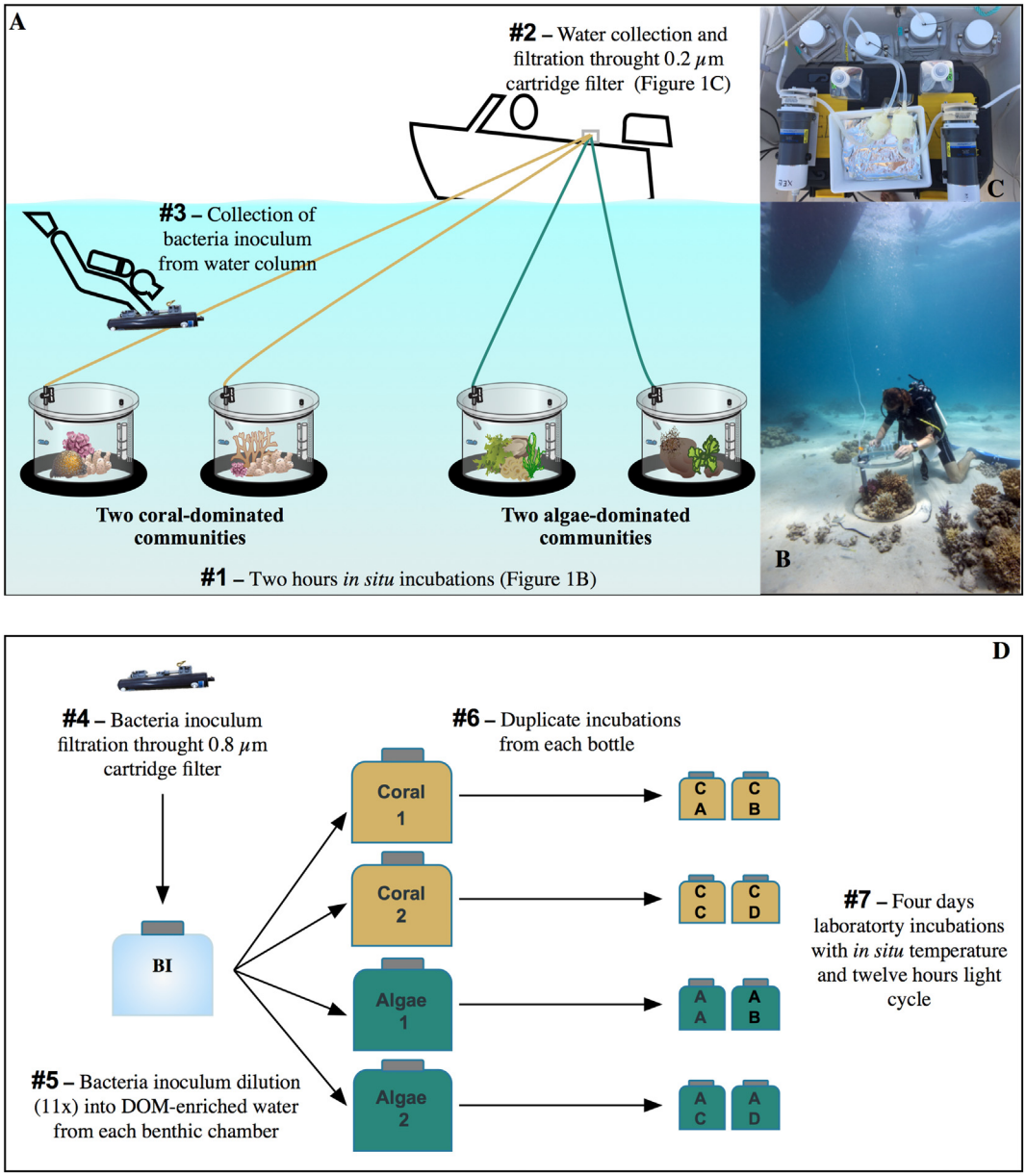

Fig. 1. Experimental setup. A) Graphical visualization of the in situ experimental procedure after the 2 h incubations of coral and algae-dominated communities; B) Picture showing the hose connected to the benthic incubation chambers for water collection; C) Picture showing the process of water filtration onboard for obtaining the coral- and algal-DOM enriched samples; D) Graphical visualization of the set-up for the laboratory incubations. Photos by H. Anlauf (B) and by L Silva (C). Graphical visualization by L. Silva and F. Roth.

2.5. Bacterial abundance and biomass

Total bacterial abundances correspond to the sum of LNA and HNA cells and were calculated after gravimetric calibration of flow cytometer flow rates. Carrying capacities were estimated as the maximum abundances and biomass recorded for each bacterial group at the plateau stage of the incubations.

Bacterial biomass (BB) was calculated using the estimation from Gundersen et al. (2002): fgC cell^{-1} = 108.8 × [Bv]$^{0.898}$ and then converted into μmol C L^{-1}, where the Bv corresponds to the biovolume. Biovolume was calculated assuming a spherical shape for all cells from the cell diameter following the empirical calibration of (Calvo-Díaz and Morán, 2006), which in turn was previously converted from the HNA and LNA side scatter (SSC, light scatter at 90°) relative to the SSC of 1 μm fluorescent beads (Molecular Probes, ref. F-13081).

2.6. Bacterial specific growth rates and growth efficiencies

The specific growth rates (μ) of the bacterial physiological groups were calculated during the corresponding exponential growth phases as the slope of the natural logarithm of bacterial abundances vs. time. The apparent activation energies (E_a in eV, Brown et al., 2004) were estimated by fitting a linear regression equation between the natural logarithm of the growth rates of all physiological groups and temperature (1/kT), where k is Boltzman's constant (8.62 × 10^{-5} eV K^{-1}) and T is water temperature (°K).

The experimental increase in total bacterial biomass (ΔBB/Δt) and the parallel changes in DOC concentration (ΔDOC/Δt) were estimated on most occasions (69%) during the exponential phase of bacterial growth. Bacterial growth efficiencies (BGE, in %), were measured as: BGE = [(ΔBB/Δt)/(-ΔDOC/Δt)] × 100, where ΔBB (μmol C L^{-1} d^{-1})

and ΔDOC (μmol C L^{-1} d^{-1}) were both estimated as the slopes of the regression lines between the respective variables and incubation time, as shown in the examples of Supplementary Fig. S1. We assumed that the remaining DOC not used for building up BB (100% - BGE) was used for bacterial respiration (BR). Bacterial respiration rates were then estimated as BR = (-ΔDOC/Δt) − (ΔBB/Δt).

Bacterial growth efficiencies were also estimated for nitrogen as BGE (%) = (ΔBBN/−ΔDON) × 100, where ΔBBN (μmol N L^{-1} d^{-1}) was converted from the ΔBB using the C:N ratio during the exponential phase of 5.2 (Vrede et al., 2002), and ΔDON (μmol N L^{-1} d^{-1}) estimated from the decrease in total DON ($DON_{initial}$ − DON_{min}).

Although the incubations were conducted under a 12 h light/12 h dark cycle, no significant phytoplankton growth was detected. With the short incubation periods and the methodology used (i.e. prefiltration through a 0.8 μm filter followed by dilution), the presence of diatoms, dinoflagellates or other large eukaryotic autotrophs was precluded. In fact, in our cytograms we could never observe picoeukaryotic cells. We did actually find *Synechococcus* cyanobacteria (on average 2.56 ± 5.74 × 10^4 cells mL^1, representing 4% of total bacteria) in the last sampling times of the experiments (i.e. after 3–4 days). *Synechococcus* cells might however have released part of their total primary production (TPP) as dissolved products (dissolved primary production, DPP) in the experimental bottles, potentially contributing an additional source of DOM for heterotrophic bacteria (Morán et al., 2002). Even using 50% of percent extracellular release (PER) [PER = DPP/TPP)], much higher than the value expected for exponentially growing phytoplankton cells (e.g. Huete-Stauffer et al., 2017; Morán et al., 2002), the low biomass increases of *Synechococcus* found in our bottles would have resulted in very low DPP values, thus representing virtually undetectable DOC and DOC extra inputs.

2.7. Data analysis

Statistical analyses were performed using JMP© Pro14 (SAS Institute) statistics software. Environmental variables and bacterial responses are first presented individually for each month and then grouped according to the in situ temperatures as warmer (i.e. >30 °C: May, July and September) and colder (i.e. <30 °C: January, March and November) months for further statistical analyses. This grouping results from the changes in ecological functions in the two communities documented during the in situ incubations (Roth, 2019). Other studies also report that the optimum temperature for corals lies below 30 °C (Anton Gamazo et al., 2020; Sawall et al., 2015). Differences in environmental variables were tested with 2-way ANOVA and Tukey HSD post-hoc pairwise comparisons when significant interactions were found between DOM exudates and months. Paired *t*-test were used to identify significant ($p < 0.05$) differences between the two different communities in warmer and colder months (see above).

2-way ANOVA and analysis of covariance (ANCOVA) were used to check whether the temperature dependence of the specific growth rates (i.e. the corresponding activation energies, E_a) differed between the bacterial physiological groups and types of DOM exudates. Pearson r coefficients are given for correlation analyses.

3. Results

3.1. Onset of laboratory incubations

Temperature showed the expected seasonality with an increase from March until September (maximum of 32.2 °C) and a subsequent decrease until January (minimum of 24.8 °C, Fig. 2A). Salinity was stable

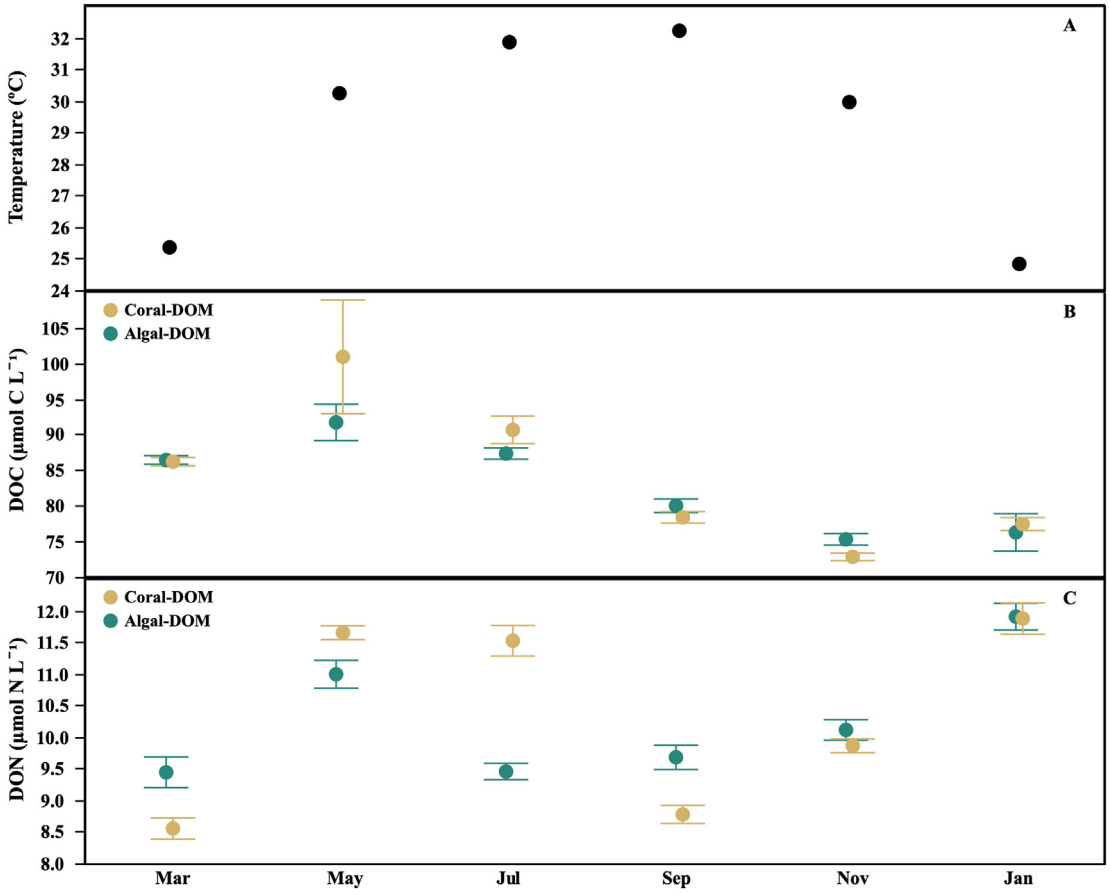

Fig. 2. Temporal dynamics of: A) Temperature; B) Average (± SE) DOC concentration; C) Average (± SE) DON concentration at the onset of coral- and algal-DOM incubations (coral-DOM - brown; algal-DOM - green).

Table 1
Monthly values at the onset of the coral- and algal-DOM incubations of nitrate and phosphate concentration, fluorescence index (FI), humification index (HIX) and biological index (BIX) and the summed Fmax values of the four DOM fluorescent components (Total FDOM). Details given in the main text. Fluorescence is reported in Raman units (RU).

	Month	Nitrate (μmol L^{-1})	Phosphate (μmol L^{-1})	FI	HIX	BIX	Total FDOM (RU)
Coral-DOM	March	1.1 ± 0.2	0.13 ± 0.02	1.45 ± 0.02	1.3 ± 0.1	1.59 ± 0.12	0.097 ± 0.004
Algal-DOM		0.8 ± 0.1	0.10 ± 0.01	1.42 ± 0.02	1.7 ± 0.2	1.34 ± 0.09	0.091 ± 0.008
Coral-DOM	May	2.3 ± 0.6	0.12 ± 0.02	1.46 ± 0.01	1.9 ± 0.1	1.13 ± 0.02	0.122 ± 0.005
Algal-DOM		1.6 ± 0.2	0.14 ± 0.02	1.47 ± 0.01	3.0 ± 0.2	0.98 ± 0.01	0.096 ± 0.001
Coral-DOM	July	1.5 ± 0.1	0.15 ± 0.01	1.48 ± 0.01	1.3 ± 0.2	1.37 ± 0.13	0.116 ± 0.008
Algal-DOM		1.4 ± 0.1	0.12 ± 0.00	1.44 ± 0.01	2.1 ± 0.1	1.11 ± 0.03	0.097 ± 0.002
Coral-DOM	September	1.4 ± 0.1	0.08 ± 0.01	1.45 ± 0.01	1.8 ± 0.2	1.10 ± 0.02	0.100 ± 0.004
Algal-DOM		1.2 ± 0.1	0.23 ± 0.03	1.46 ± 0.02	3.0 ± 0.3	0.98 ± 0.02	0.084 ± 0.008
Coral-DOM	November	1.4 ± 0.2	0.16 ± 0.03	1.51 ± 0.04	1.6 ± 0.3	1.10 ± 0.03	0.097 ± 0.009
Algal-DOM		1.5 ± 0.1	0.35 ± 0.05	1.44 ± 0.03	1.9 ± 0.3	1.02 ± 0.01	0.087 ± 0.005
Coral-DOM	January	1.5 ± 0.3	0.13 ± 0.01	1.43 ± 0.02	1.4 ± 0.1	1.13 ± 0.10	0.086 ± 0.008
Algal-DOM		1.4 ± 0.4	0.15 ± 0.03	1.47 ± 0.01	0.9 ± 0.4	1.13 ± 0.04	0.085 ± 0.005

throughout the study period, with values ranging from 39.6 (March and July) to 40.1 (November).

Nitrate concentrations were generally higher in coral- than in algal-DOM seawater, with values ranging from 1.08 to 2.29 μmol L^{-1} and from 0.81 to 1.64 μmol L−1, respectively. However, they displayed a similar temporal variability (Table 1) and differences were not significant between and for both DOM exudates. The opposite trend was observed for phosphate, particularly from September to January, with minima of 0.08 and 0.10 and maxima of 0.16 and 0.35 μmol L^{-1}, in coral- and algal-DOM, respectively (Table 1). No significant differences were found in coral-DOM phosphate concentration, while algal-DOM showed significantly higher phosphate concentrations in November compared with the other months, except September (2-way ANOVA, Tukey HSD, $p < 0.05$, $n = 24$). Phosphate concentrations significantly differed between the two DOM exudates in September and November (2-way ANOVA, Tukey HSD, $p < 0.005$, $n = 6$).

Initial DOC concentrations showed a clear seasonal pattern (Fig. 2B). Minimum values were observed in November (72.8 and 75.3 μmol C L^{-1} in coral- and algal-DOM, respectively) and maximum in May (100.8 and 91.7 μmol C L^{-1} in coral- and algal-DOM, respectively). DOC concentrations in coral-DOM were significantly higher than in algal-DOM in May were found (2-way ANOVA, Tukey HSD, $p < 0.05$, $n = 24$)., Significant differences between months in algal-DOM DOC concentration were found for the period between May and November (2-way ANOVA, Tukey HSD, $p < 0.05$, $n = 24$). However, bulk DOC concentrations were not significantly different between the two DOM exudates. DON concentrations showed minimum values in March (8.55 and 9.44 μmol N L^{-1}, coral- and algal-DOM, respectively) and maximum in January (11.68 and 11.89 μmol N L^{-1}) (Fig. 2C). In coral-DOM, DON concentrations were significantly higher in May, July and January (2-way ANOVA, Tukey HSD, $p < 0.05$, $n = 24$), while only January had a significantly higher value in algal-DOM (2-way ANOVA, Tukey HSD, $p < 0.005$, $n = 24$). We found significant differences in DON concentration between the two DOM exudates in July and September, with higher values in Coral- and Algal-DOM, respectively (2-way ANOVA, Tukey HSD, $p < 0.005$, $n = 6$). No significant differences were found for bulk DOC and DON concentrations between the two exudates in warmer and colder months.

Total FDOM (sum of Fmax from all components) ranged from 0.086 to 0.122 R.U. in coral-DOM and from 0.083 to 0.097 R.U. in algal-DOM (Table 1). We found significantly higher total FDOM values in coral-DOM than in algal-DOM (paired *t*-test, $p = 0.0171$, $n = 6$). In coral-DOM, the protein-like components C3 (Tyrosine-like) and C4 (Tryptophan-like) showed higher fluorescence intensities year-round. In algal-DOM, C3 also showed consistently higher fluorescence intensities, but, the fluorescence intensities of the other components showed greater seasonal variability (Supplementary Table S2). The contribution of protein-like components to total FDOM was significantly higher in coral-DOM than in algal-DOM (paired t-test, $p = 0.001$, n = 6), ranging from 53.5 to 62.0% and from 44.4 to 55.8%, respectively. The fluorescence index (FI) varied little between DOM exudates, ranging from 1.38 to 1.61. FI index suggests a presence of a mix of terrestrial-like (FI ~ 1.2) and marine microbial (FI ~ 1.8). The biological index (BIX), indicative of freshly produced DOM or recent biological activity, was significantly higher in coral-DOM (paired *t*-test, $p = 0.0173$, n = 6), with values ranging from 1.13 to 1.60 compared with the algal-DOM (0.98–1.34). The humification index (HIX), which is mostly linked with humic-like substances released by microbial remineralization, ranged from 1.32 to 1.93 in coral-DOM and from 1.58 to 3.03 in algal-DOM (Table 1). Significantly higher HIX values were found in the algal-DOM (paired *t*-test, $p = 0.0150$, $n = 6$), especially during the warmer months (Fig. 4A).

Initial bacterial abundances in our experiments (i.e. after dilution) were expectedly one order of magnitude lower, ranging from 1.7 ± 0.1 × 10^4 cells mL^{-1} in March to 5.7 ± 0.2 × 10^4 cells mL^{-1} in November, equivalent to 1.9 ± 0.2 × 10^5 cells mL^{-1} and 6.3 ± 0.2 × 10^5 cells mL^{-1} in the original seawater.

3.2. DOM and nutrient fluxes

DOC consumption was observed year-round in the laboratory incubations in both DOM exudates (Fig. 3A). Maximum rates (ΔDOC/Δt) were reached in May for both DOM exudates while minimum values were measured in September for algal-DOM and in November for coral-DOM. ΔDOC/Δt ranged from 1.18 to 6.00 μmol C L^{-1} d^{-1} for coral-DOM and from 1.08 to 3.33 μmol C L^{-1} d^{-1} for algal-DOM (Fig. 3A). In spite of the high variability, mean DOC consumption rates were significantly higher in coral-DOM during the warmer months (paired *t*-test, $p = 0.011$, $n = 3$, Fig. 4B). As expected, DON was also consistently consumed during the incubations with ΔDON/Δt values ranging from −0.40 to −0.97 μmol N L^{-1} d^{-1} in coral-DOM and from −0.48 to −0.91 μmol N L^{-1} d^{-1} in algal-DOM, with no significant differences (Table 2).

The FDOM components C2, C3, C4 and C5 were regularly consumed throughout the year, while C1 was mostly produced (Supplementary Fig. S2). On an annual basis, the protein-like components C3 and C4 were consumed at higher rates in both DOM exudates. However, none of the consumption rates of the FDOM components showed significant differences between the two DOM exudates (Supplementary Fig. S2).

Consumption of phosphate was observed for most of the year in both DOM exudates (Table 2), but it was more evident in coral-DOM, with an annual average of −0.014 ± 0.032 μmol L^{-1} d^{-1}. In contrast, phosphate dynamics in algal-DOM varied greatly, resulting in an annual average weak production rather than consumption of 0.029 ± 0.133 μmol L^{-1} d^{-1} (Table 2).

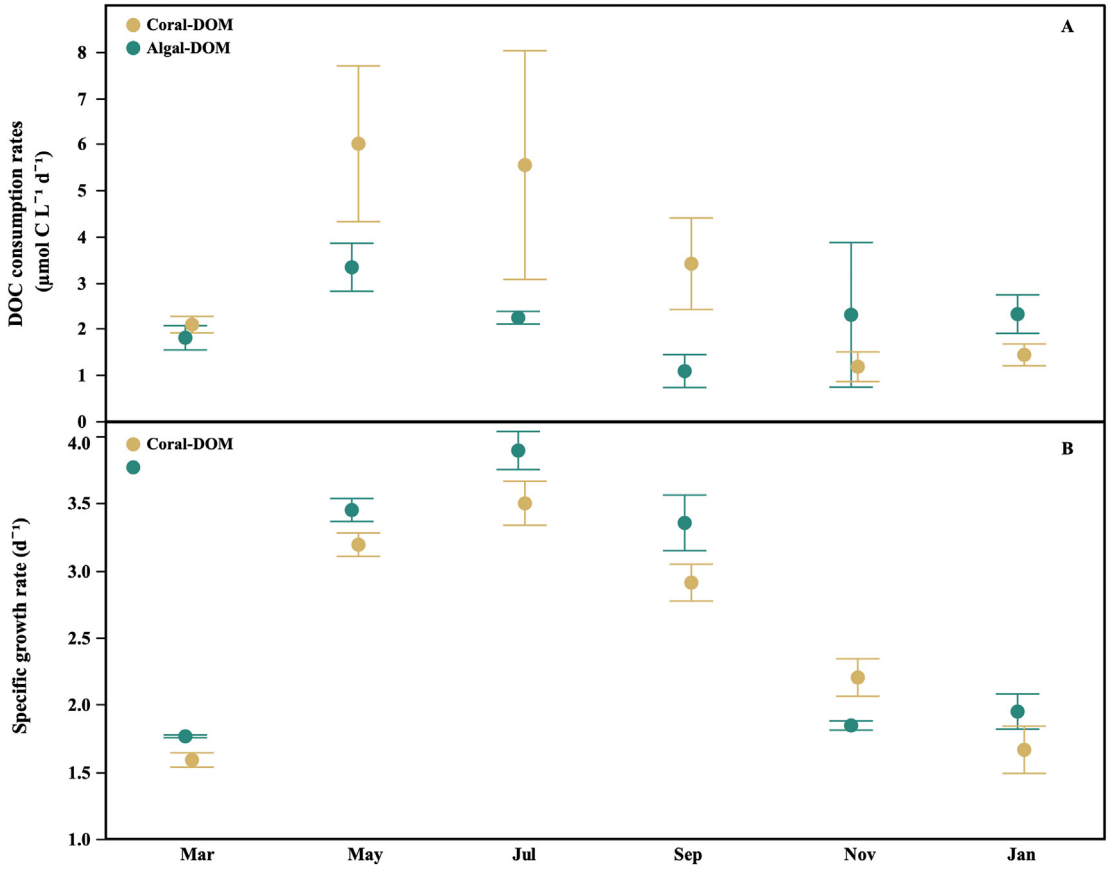

Fig. 3. Temporal distribution of: A) Average (± SE) of DOC consumption rates (µmol C L^{-1} d^{-1}); B) Average (± SE) of total bacteria specific growth rates (d^{-1}) during coral- and algal-DOM incubations (coral-DOM - brown; algal-DOM - green).

3.3. Bacterial growth rates and efficiencies

Heterotrophic bacterial growth rates showed very similar seasonal patterns with both DOM exudates. Specific growth rates of the total (i.e. LNA + HNA cells) bacterial community showed similar minima in March (1.6 vs. 1.8 d^{-1}) and peaked in July (3.5 vs. 3.9 d^{-1}) in coral- and algal-DOM, respectively (Fig. 3B). Notwithstanding the similar temporal dynamics, bacterial specific growth rates were significantly higher in algal-DOM during the warmer months (paired *t*-test, $p = 0.022$, $n = 3$ - Fig. 4C). The specific growth rates of HNA cells were significantly higher than those of LNA cells and the other physiological groups (Supplementary Fig. S3). Algal-DOM resulted in significantly higher specific growth rates of HNA bacteria compared to coral-DOM (paired *t*-test, $p < 0.05$, $n = 6$), but no differences were found in the remaining physiological groups (Supplementary Fig. S3).

With all data pooled, total specific growth rates were strongly and positively correlated with temperature in coral- ($r = 0.74$, $p < 0.0001$, $n = 24$) and algal-DOM ($r = 0.69$, $p = 0.0002$, $n = 24$), resulting in apparent activation energies of 0.65 (±0.08) and 0.60 (±0.10) eV, respectively (Fig. 5A). A positive correlation of total specific growth rates was also found with the initial DOC concentrations for both DOM exudates s ($r = 0.57$, $p = 0.0033$, for coral-DOM; $r = 0.68$, $p = 0.0002$, for algal-DOM, $n = 24$, Fig. 5B).

Considering the different physiological groups, the activation energy of HNA cells was lower in both DOM exudates (0.51 and 0.31 eV coral- and algal-DOM, respectively) than the other physiological groups (Table 3). However, significant differences were only found between HNA and CTC+ cells (ANCOVA, $p = 0.047$ for coral-DOM and $p = 0.0106$ for algal DOM, $n = 40$). No significant differences were found in Ea values of the different physiological groups or the total between the DOM exudates.

Contrary to specific growth rates, no clear seasonal patterns were found in bacterial carrying capacities in both DOM exudates. The carrying capacities ranged from 3.34 to 6.50 × 10^5 cells mL^{-1} for coral-DOM, and from 3.98 to 7.95 × 10^5 cells mL^{-1} for algal-DOM (Supplementary Table S3).

The rates of increase in heterotrophic bacterial biomass (ΔBB/Δt) concomitant to the above-mentioned DOC consumption rates ranged from 0.13 to 0.32 µmol C L^{-1} d^{-1} in coral-DOM and from 0.14 to 0.48 µmol C L^{-1} d^{-1} in algal-DOM (Table 2), resulting in mean bacterial growth efficiency (BGE) estimates of 11.8% and 13.0% respectively. Bacterial growth efficiencies peaked in November for coral-DOM (25.2 ± 6.0%) and September for algal-DOM (19.9 ± 3.2%), with respective minima in July (6.6 ± 2.4%) and January (6.7 ± 1.2%) (Fig. 6A). We observed a positive correlation of BGE with in situ temperature for algal-DOM ($r = 0.54$, $p = 0.009$, $n = 22$). In the warmer months, BGE was significantly higher in algal- than in coral-DOM (paired *t*-test, $p = 0.020$, $n = 3$ - Fig. 4D). Estimated respiration rates (BR = (-ΔDOC/Δt) – (ΔBB/Δt)) ranged between 0.94 (November) and 5.68 µmol C L^{-1} d^{-1} (May) for coral-DOM and from 0.89 (September) to 2.85 µmol C L^{-1} d^{-1} (May) for algal-DOM (Fig. 6B). Similarly to bacterial production (i.e. ΔBB/Δt), bacterial respiration in coral-DOM was significantly higher in warmer (May–September) than in colder months (ANOVA, $p = 0.16$, $n = 6$). Due to changes in BGE (Fig. 4D, Fig. 6A), Bacterial respiration in coral-DOM was positively correlated with the maximum abundance attained by the fraction of actively respiring or CTC+ cells ($r = 0.57$, $p = 0.0101$, $n = 19$).

Compared to DOC, DON-based growth efficiencies (measured by DON consumptions and increases in bacterial biomass in carbon

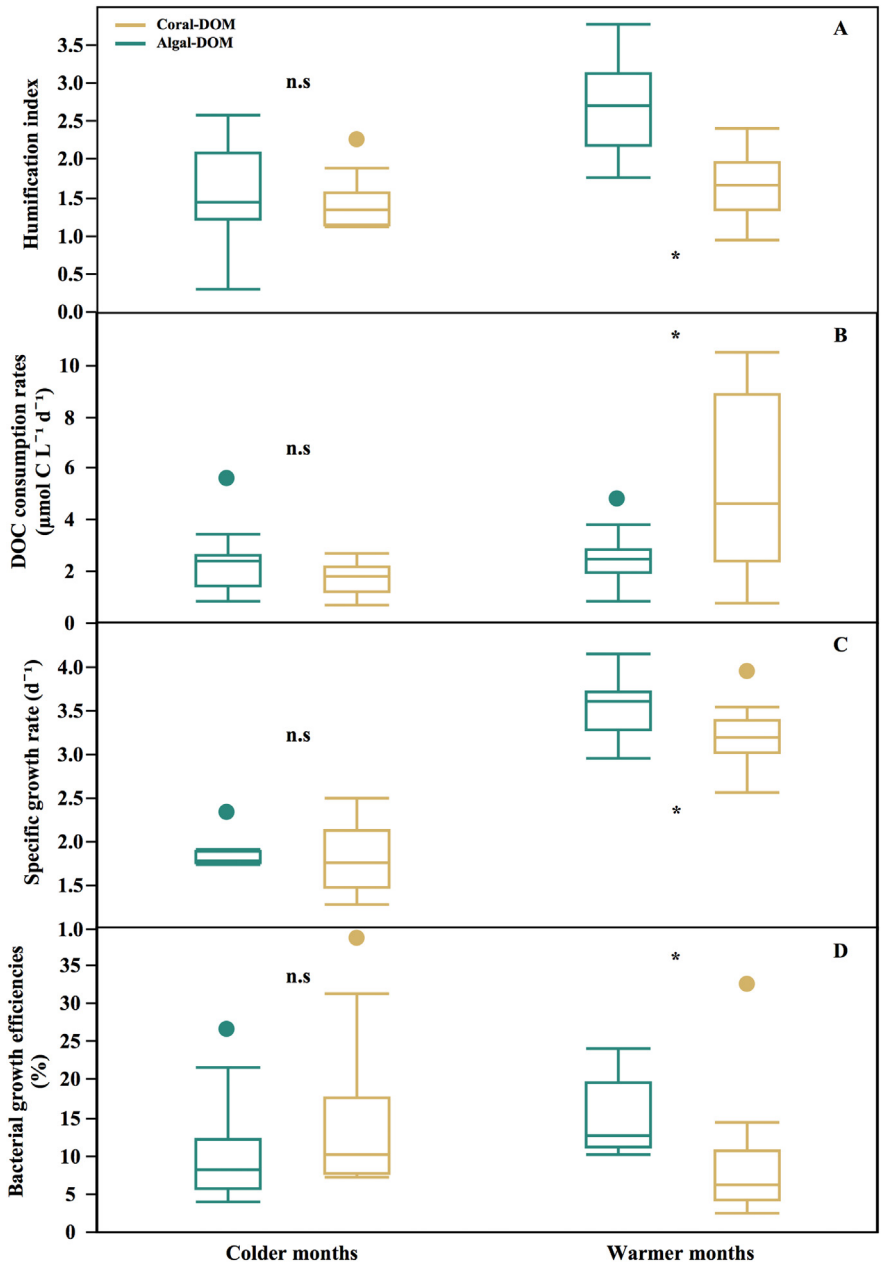

Fig. 4. Box plots of: A) humification index; B) DOC consumption rates (µmol C L^{-1} d^{-1}); C) specific growth rates (d-1); D) bacterial growth efficiencies (%) during the colder months (< 30 °C) and warmer months (> 30 °C) during coral- and algal-DOM incubations (coral-DOM - brown; algal-DOM - green). The horizontal line inside the boxes represents the median, the boxes extend from the 25% to the 75% quartile of the data distribution, and the horizontal lines outside the boxes indicate the 5% and 95% quartiles. Paired t-tested were conducted for each temperature range between DOM exudates (n.s – non significant, * $p < 0.05$).

converted to nitrogen) were seasonally less variable and lower, with values ranging from 5.4 to 13.2% in coral-DOM and from 4.9 to 18.8% in algal-DOM (Table 2).

4. Discussion

To our knowledge, this study is the first systematic temporal assessment of the effects of different DOM exudates resulting from critical changes in the dominant benthic functional groups (i.e. healthy corals vs. corals overgrown by algae) on the standing stocks and activity of heterotrophic bacterioplankton, the most abundant planktonic organisms, in overlying waters. While previous works focused on temporal snapshots of the effects of DOM released by individual species of benthic primary producers on planktonic microbes (Haas et al., 2011, 2013; Nelson et al., 2013; Silveira et al., 2019), here, we present the first detailed study with natural communities incorporating the entire annual cycle.

Similar to other studies (Haas et al., 2011, 2013; Silveira et al., 2015), a higher amount of DOC per square meter of reef was produced in the algae-dominated communities than in those dominated by corals (721 ± 59 vs. 601 ± 74 µmol m^{-2} h^{-1}, Roth et al., submitted). However, at the onset of our laboratory incubations, bulk DOC concentrations were not significantly different and showed a similar seasonal pattern for the two reef communities (Fig. 2B). We did find, however, a higher humification index (HIX) in the algal-DOM, which likely resulted from an increase of humic-like substances during microbial remineralization (Calleja et al., 2019; Catalá et al., 2015), and consequent depletion of freshly produced DOC (as shown by lower BIX values, Table 1). This higher amount of humic-like components in algal-DOM is in line with Quinlan et al. (2018), and indicates that although total DOC

Table 2
Monthly consumption (<0) or production (>0) rates of inorganic phosphate (ΔPhosphate/Δt), DON (ΔDON/Δt), increase in heterotrophic bacterial biomass in carbon (ΔBBC/Δt), and nitrogen (ΔBBN/Δt) content, and bacterial growth efficiency in terms of nitrogen incorporation (BGE_N) within the incubations for both treatments.

	Month	ΔPhosphate/Δt (μmol L^{-1} d^{-1})	ΔDON/Δt (μmol N L^{-1} d^{-1})	ΔBBC/Δt (μmol C L^{-1} d^{-1})	ΔBBN/Δt (μmol N L^{-1} d^{-1})	BGE_N (%)
Coral-DOM	March	−0.018 ± 0.012	−0.52 ± 0.08	0.18 ± 0.01	0.034 ± 0.001	7.2 ± 1.4
Algal-DOM		−0.024 ± 0.012	−0.91 ± 0.25	0.17 ± 0.01	0.033 ± 0.001	4.4 ± 1.1
Coral-DOM	May	−0.025 ± 0.004	−0.97 ± 0.15	0.32 ± 0.05	0.062 ± 0.005	6.7 ± 0.7
Algal-DOM		−0.021 ± 0.021	−0.50 ± 0.05	0.48 ± 0.04	0.092 ± 0.004	18.8 ± 2.1
Coral-DOM	July	−0.030 ± 0.017	−0.40 ± 0.09	0.25 ± 0.02	0.049 ± 0.001	14.0 ± 3.0
Algal-DOM		0.009 ± 0.015	−0.65 ± 0.06	0.25 ± 0.02	0.049 ± 0.001	7.7 ± 0.8
Coral-DOM	September	0.028 ± 0.022	−0.56 ± 0.12	0.25 ± 0.04	0.047 ± 0.004	7.5 ± 1.1
Algal-DOM		0.273 ± 0.061	−0.48 ± 0.10	0.22 ± 0.07	0.042 ± 0.006	11.4 ± 4.5
Coral-DOM	November	−0.040 ± 0.015	−0.50 ± 0.15	0.24 ± 0.05	0.046 ± 0.004	11.3 ± 2.4
Algal-DOM		−0.076 ± 0.025	−0.73 ± 0.01	0.19 ± 0.03	0.037 ± 0.003	5.1 ± 0.4
Coral-DOM	January	−0.005 ± 0.006	−0.50 ± 0.06	0.13 ± 0.04	0.025 ± 0.004	5.4 ± 1.5
Algal-DOM		0.005 ± 0.013	−0.58 ± 0.07	0.14 ± 0.02	0.027 ± 0.002	4.9 ± 0.6

concentration was not significantly different, the actual compounds present differed between the two communities. Algae-dominated communities are often also associated with a high amount of sponges and other benthic filter feeders (Abele and Patton, 1976) that utilize DOC together with particulate organic carbon (Rix et al., 2017, 2018). Hence, in spite of the higher production rates in algae-dominated systems, its lability, suggested by higher HIX, likely led to faster DOC remineralization and decrease in DOC concentrations (Haas et al., 2016; Nelson et al., 2011) at the onset of our incubations.

The specific growth rates of total heterotrophic bacteria reported here were notably higher (2.2-fold, on average) than those previously measured at a nearby (~7 km southwest of the study site) coastal station with similar DOC concentrations (73.8–98.2 μmol C L^{-1}), obtained in experiments conducted with predator-free water (Silva et al., 2019). Even though the increase in substrates available for each bacterium (by 11× dilution) led to this huge increase in specific growth rates, the carrying capacities eventually found for surface bacterioplankton communities overlying the sampled coral reef communities (on average 5.2 and 5.5 × 10^5 cells mL^{-1} for coral- and algal-DOM, respectively) were lower than the annual mean values found in the aforementioned study (7.3 × 10^5 cells mL^{-1}), suggesting reef waters were subject to higher nutrient limitation than the shallow waters of KAUST Harbor. In fact, while bacterial nitrogen requirements seem to have been fulfilled by DON, we observed a consistent consumption of phosphate during the exponential growth phase, especially in the coral-DOM (Table 2), in agreement with the low concentrations found year-round (<0.16 μmol L^{-1}). This consistent phosphate consumption was also previously observed in coastal waters of the Red Sea (Silva et al., 2019), suggesting a phosphorus limitation in Red Sea waters. The consistently higher phosphate uptake rates in coral-DOM than in algal-DOM agrees with the strong phosphorus limitation reported for other tropical corals reefs (Ezzat et al., 2016).

Total bacterial specific growth rates showed a similar seasonal pattern for the two different DOM sources but, similar to other tropical systems (Haas et al., 2011; Nelson et al., 2013), values were higher in the algal-DOM, especially during the warmer months. The apparent activation energies of specific growth rates, an indication of their temperature dependence (Huete-Stauffer et al., 2015; Morán et al., 2020), showed values close and statistically indistinguishable to those predicted for heterotrophic organisms (0.65 eV) by the metabolic theory of ecology (Brown et al., 2004). This indicates that under resource-sufficiency (expected by our dilution experiments), warmer conditions will enhance bacterial growth similarly in both benthic communities. Higher activation energies can also be interpreted as the presence of more complex DOM and less susceptible to bacterial uptake (Lønborg et al., 2016a, 2019; Sierra, 2012). Indeed, the slightly higher activation energies in coral-DOM for all the physiological groups except *Live* cells (Table 3) could hint at a possible higher complexity of coral-DOM. Even though higher specific growth rates were found for algal-DOM, particularly during the warmer months, the activation energies did not significantly differ between the two DOM sources, suggesting that processes other than temperature may drive the actual differences in bacterial growth.

Contrary to what was previously reported (e.g. Smith et al., 2006; Wild et al., 2010; Haas et al., 2011, 2013, 2016; Nelson et al., 2013), for most of the year, we detected higher DOC consumption rates and higher percentages of DOC consumed in coral- than in algal-DOM. However, the amount of DOC consumed or bioavailable DOC does not inform us of its subsequent fate in terms of bacterial biomass increase (Lønborg et al., 2019; Silva et al., 2019). Although not statistically significant, the average consumption rates of fluorescence components were also slightly higher in coral-DOM year-round (see Supplementary Fig. S2). The higher lability of dissolved compounds present in our coral-DOM laboratory incubations could be related to higher bacterial remineralization, shown by the higher HIX, of the algal labile DOM during in situ incubations originating an apparently more refractory DOC at the onset of the incubations.

As a summary of the ability of heterotrophic prokaryotes to produce new biomass from consumed DOM, bacterial growth efficiency (BGE) allows us to rapidly assess their contribution to carbon fluxes in pelagic food webs (Alonso-Sáez et al., 2008; Carlson et al., 2007; del Giorgio and Cole, 1998). Our mean BGE values in coral-DOM (12 ± 2.%, Fig. 6A) were lower than those found in French Polynesia in incubations with *Porites* exudates in September (18 ± 8% - Nelson et al., 2013) but higher than those found in Brazil in February (3 ± 2% and 5 ± 2% - Silveira et al., 2015). Mean BGE in algal-DOM values (13 ± 4%, Fig. 6A) was within the range reported in the above-mentioned studies (6–20% for different algal species, Haas et al., 2011; Nelson et al., 2013; Silveira et al., 2015). These growth efficiencies indicate that 74 to 93% of the carbon taken up was respired. Overall, our BGE values with enriched DOM were also substantially higher than in the nearby coastal embayment (annual mean 6 ± 1% - Silva et al., 2019). Temperature and DOM lability are among the major factors affecting BGE (e.g. Lemée et al., 2002; Carlson et al., 2007; Alonso-Sáez et al., 2008; Silva et al., 2019). While coral exudates are usually richer in lipids and proteins, algal exudates are mostly composed by labile carbohydrates (Haas and Wild, 2010; Nelson et al., 2013; Quinlan et al., 2018). The different composition of the dissolved compounds released by the two communities likely influence the microbial utilization of lower efficient carbon metabolism pathways (e.g. Entner–Doudoroff and pentose phosphate pathways) in algal exudates (Haas et al., 2016). In fact, lower bacterioplankton growth efficiencies have been reported in algal exudates (Haas et al., 2011; Nelson et al., 2013; Silveira et al., 2015). Temperature, which positively correlated with BGE in a recent study in coastal waters of the central Red Sea (Silva et al., 2019), was found to enhance BGE only in algal-DOM. Thus, the overall lower bacterial growth efficiencies when using coral DOM (although differences were only significant in the warmer period from

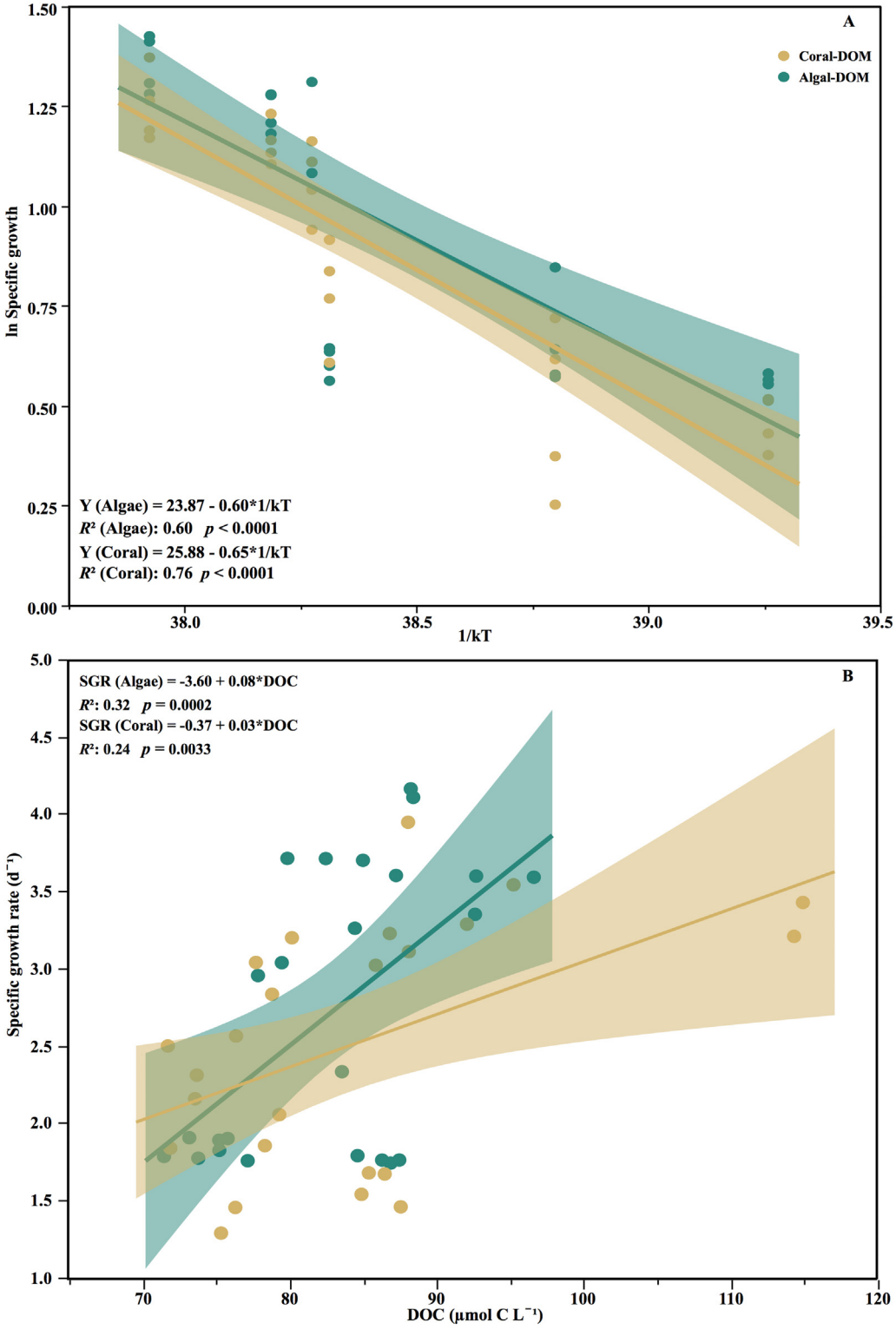

Fig. 5. A) Arrhenius relationship between the natural logarithm of total bacteria specific growth rates and the inverted temperature (1/kT) where k = Boltzmann's constant (8.617×10^{-5} eV K^{-1}) and T = water temperature (Kelvin); B) Relationship between total bacteria specific growth rates (d^{-1}) with DOC concentrations (µmol C L^{-1}) at the onset of the coral- and algal-DOM incubations (coral-DOM - brown; algal-DOM - green).

May to September, Figs. 3B, 4D), suggests that the metabolites released by healthy coral communities represent a relatively lower-quality substrate, in the sense that DOC was rapidly utilized by bacteria but poorly accumulated into their biomass, ultimately leading to higher bacterial respiration rates. Interestingly, we found significantly higher carrying capacities of actively respiring (CTC+) cells in the coral-DOM during that season (Supplementary Table S3). The 2-fold higher abundances of CTC+ cells, which were also associated with bulk microbial respiration in coastal waters (Sherr et al., 1999; Smith, 1998), reinforce the hypothesis of higher bacterial respiration with coral-DOM during summer.

Table 3
Apparent activation energy (*Ea*) of the growth rates (μ) of the four physiological groups of heterotrophic bacteria distinguished during the coral- and algal-DOM incubations; R^2 = coefficient of determination; p = p-value.

	μHNA		μLNA		μ*Live*		μCTC+	
	Coral	Algal	Coral	Algal	Coral	Algal	Coral	Algal
Ea (eV)	0.51	0.31	0.67	0.43	0.54	0.58	1.11	1.08
R^2	0.57	0.41	0.4	0.13	0.64	0.6	0.33	0.62
p	<0.0001	0.0008	0.0016	0.0872	<0.0001	<0.0001	0.0078	<0.0001

It is also important to mention here possible inconsistencies in the methodology used in the different studies. Firstly, while the natural light and dark cycle incubations are a better approach to represent the natural conditions, they could potentially be affected by some artificial supply of DOC if picophytoplankton grows substantially in the incubations, which it was not the case in our incubations. On the other hand, the common use of dark incubations neglects the potential role of photoheterotrophic bacteria in carbon fluxes, which can be substantial (Arandia-Gorostidi et al., 2020; Ferrera et al., 2017). Secondly, changes in cell size were not considered in previous studies (Haas et al., 2011; Nelson et al., 2013; Silveira et al., 2015) but bacterial cells have been recently described to become larger when stimulated by algae than corals (Silveira et al., 2019). Silveira et al. (2019) further suggested that bacteria stimulated by algal products might have a possible overflow metabolism that results in a decoupling of DOC from oxygen consumption and might lead to an increase in bacterial biomass that can affect trophic interactions at reef-scale (Haas et al., 2016; Silveira et al., 2015).

Coral- and algae-dominated reef communities are extremely complex and dynamic systems, and despite recent efforts, their biogeochemistry are still poorly understood. More seasonal assessments at the community-level are needed to better understand how ongoing and future coral-algae regime shifts will affect DOM composition and its subsequent processing by pelagic heterotrophic bacteria and archaea. Our results suggest that surface heterotrophic bacterioplankton growth in the Red Sea may be fostered when exposed to DOM released by reef algae. Considering that, as part of the natural assemblage, there are opportunistic bacteria associated with coral diseases (e.g. Dinsdale and Rohwer, 2011; Barott et al., 2012; Nelson et al., 2013; Cárdenas et al., 2018), the overall higher growth rates of heterotrophic bacterioplankton in algal-DOM reported here could enhance coral degradation and result in a positive feedback of algal overgrowth in the future, as previously shown (Barott and Rohwer, 2012; Nelson et al., 2013) and in accordance with the DDAM model.

While algae exudates are commonly seen as more labile, the faster uptake of coral DOC in our experiments led to lower bacterial growth efficiencies. Contrary to other tropical systems, the higher growth efficiencies in the algal exudates suggest a potentially larger transfer of carbon bacterial up the pelagic food web. In agreement with this

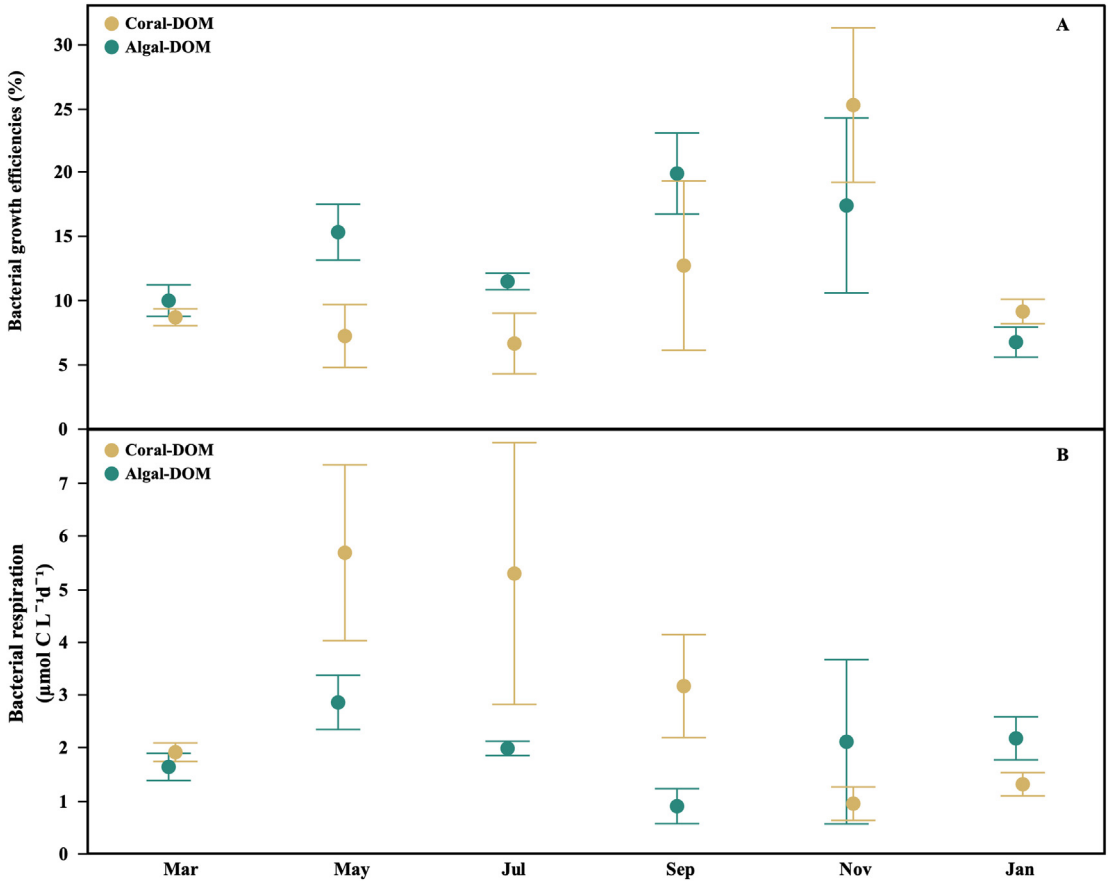

Fig. 6. Temporal distribution of: A) Average (±SE) of bacterial growth efficiencies (%); B) Average (± SE) of bacterial respiration (μmol C L^{-1} d^{-1}) during coral- and algal-DOM incubations (coral-DOM - brown; algal-DOM - green).

hypothesis, Roth et al. (submitted) observed that high temperatures led to changes in several ecological functions such as net productivity or carbon and carbonate cycles in coral- vs algae-dominated communities during in situ experiments. Hence, it is not surprising that the major differences in bacterial responses also occurred during the warmest period (see Fig. 4). Following our results, with the indubitable increase of temperature of tropical regions in the last decades (e.g. Chaidez et al., 2017; Heron et al., 2016; Spalding and Brown, 2015) a competitive advantage and expansion of algae-dominated communities over coral-dominated benthos systems might be expected. Although it was not investigated here, this expansion algae-dominated communities might also favor the growth of copiotrophic bacteria and increase virulence factors in coral reef systems (Cárdenas et al., 2018; Morrow et al., 2011; Nelson et al., 2013). Finally, if corals are increasingly being replaced by algae in tropical reefs, this shift might stimulate bacterioplankton assemblages, ultimately resulting in further coral reef degradation.

Supplementary data to this article can be found online at https://doi.org/10.1016/j.scitotenv.2020.141628.

CRediT authorship contribution statement

Luis Silva: Conceptualization, Investigation, Methodology, Formal analysis, Writing - original draft. **Maria Ll. Calleja:** Conceptualization, Methodology, Writing - review & editing, Formal analysis. **Snjezana Ivetic:** Methodology, Investigation. **Tamara Huete-Stauffer:** Formal analysis, Writing - review & editing. **Florian Roth:** Resources, Methodology, Investigation, Writing - review & editing. **Susana Carvalho:** Resources, Writing - review & editing. **Xosé Anxelu G. Morán:** Conceptualization, Methodology, Supervision, Writing - review & editing, Project administration.

Declaration of competing interest

The authors declare that they have no known competing financial interests or personal relationships that could have appeared to influence the work reported in this paper.

Acknowledgments

We gratefully acknowledge Miguel Viegas, João Curdia and Rodrigo Villalobos who aided us with laboratory and fieldwork and KAUST Coastal and Marine Resources Core Lab (CMOR) for their diligent fieldwork assistance. Funding: This project was supported by King Abdullah University of Science and Technology (KAUST) through the baseline research funding provided to X.A.G. Morán, S. Carvalho was financially supported by Saudi Aramco/KAUST Center for Marine Environmental Observations. This research was undertaken in accordance with the policies and procedures of KAUST. Permissions relevant for KAUST to undertake the research have been obtained from the applicable governmental agencies in the Kingdom of Saudi Arabia.

References

Abele, L.G., Patton, W.K., 1976. The size of coral heads and the community biology of associated decapod crustaceans. J. Biogeogr. 35–47.

Alonso-Sáez, L., Vázquez-Domínguez, E., Cardelús, C., Pinhassi, J., Sala, M.M., Lekunberri, I., Balagué, V., Vila-Costa, M., Unrein, F., Massana, R., Simó, R., Gasol, J.M., 2008. Factors controlling the year-round variability in carbon flux through bacteria in a coastal marine system. Ecosystems 11, 397–409. https://doi.org/10.1007/s10021-008-9129-0.

Ammerman, J.W., Fuhrman, J.A., Hagstrom, A., Azam, F., Hagström, A., Azam, F., 1984. Bacterioplankton growth in seawater: I. growth kinetics and cellular characteristics in seawater cultures. Mar. Ecol. Prog. Ser. Oldend. 18, 31–39.

Anton Gamazo, A., Randle, J.L., Garcia, F.C., Rossbach, S., Ellis, J.I., Weinzierl, M., Duarte, C.M., 2020. Differential thermal tolerance between algae and corals may trigger the proliferation of algae in coral reefs.

Arandia-Gorostidi, N., González, J.M., Huete-Stauffer, T., Ansari, M.I., Morán, X.A.G., Alonso-Sáez, L., 2020. Light supports cell-integrity and growth rates of taxonomically diverse coastal photoheterotrophs. Environ. Microbiol. 1462-2920, 15158. https://doi.org/10.1111/1462-2920.15158.

Atkinson, M.J., Falter, J.L., Black, K.D., Shimmield, G.B., 2003. Biogeochemistry of Marine Systems. Coral Reefs. Blackwell, Oxford, pp. 40–64.

Azam, F., Malfatti, F., 2007. Microbial structuring of marine ecosystems. Nat. Rev. Microbiol. 5, 782–791. https://doi.org/10.1038/nrmicro1747.

Azam, F., Fenchel, T., Field, J.G., Gray, J.S., Meyer-Reil, L.A., Thingstad, F., 1983. The ecological role of water column microbes in the sea. Mar. Ecol. Prog. Ser. 10, 257–263 (doi: citeulike-article-id:7826056).

Barott, K.L., Rohwer, F.L., 2012. Unseen players shape benthic competition on coral reefs. Trends Microbiol. 20, 621–628. https://doi.org/10.1016/j.tim.2012.08.004.

Barott, K., Smith, J., Dinsdale, E., Hatay, M., Sandin, S., Rohwer, F., 2009. Hyperspectral and physiological analyses of coral-algal interactions. PLoS One 4. https://doi.org/10.1371/journal.pone.0008043.

Barott, K.L., Williams, G.J., Vermeij, M.J.A., Harris, J., Smith, J.E., Rohwer, F.L., Sandin, S.A., 2012. Natural history of coral-algae competition across a gradient of human activity in the Line Islands. Mar. Ecol. Prog. Ser. 460, 1–12. https://doi.org/10.3354/meps09874.

Bellwood, D.R., Hughes, T.P., Folke, C., Nyström, M., 2004. Confronting the coral reef crisis. Nature 429, 827–833. https://doi.org/10.1038/nature02691.

Berumen, M.L., Arrigoni, R., Bouwmeester, J., Terraneo, T.I., Benzoni, F., 2019a. Corals of the Red Sea. Coral Reefs of the Red Sea. Springer, pp. 123–155.

Berumen, M.L., Voolstra, C.R., Daffonchio, D., Agusti, S., Aranda, M., Irigoien, X., Jones, B.H., Morán, X.A.G., Duarte, C.M., 2019b. The Red Sea: environmental gradients shape a natural laboratory in a nascent ocean. Coral Reefs of the Red Sea. Springer, pp. 1–10.

Brown, J.H., Gillooly, J.F., Allen, A.P., Savage, V.M., West, G.B., 2004. Toward a metabolic theory of ecology. Ecology 85, 1771–1789.

Calleja, M.L., Al-Otaibi, N., Morán, X.A.G., 2019. Dissolved organic carbon contribution to oxygen respiration in the central Red Sea. Sci. Rep. 9, 4690. https://doi.org/10.1038/s41598-019-40753-w.

Calvo-Díaz, A., Morán, X.A.G., 2006. Seasonal dynamics of picoplankton in shelf waters of the southern Bay of Biscay. Aquat. Microb. Ecol. 42, 159–174. https://doi.org/10.3354/ame042159.

Cárdenas, A., Neave, M.J., Haroon, M.F., Pogoreutz, C., Rädecker, N., Wild, C., Gärdes, A., Voolstra, C.R., 2018. Excess labile carbon promotes the expression of virulence factors in coral reef bacterioplankton. ISME J 12, 59–76. https://doi.org/10.1038/ismej.2017.142.

Carlson, C.A., Del Giorgio, P.A., Herndl, G.J., 2007. Microbes and the dissipation of energy and respiration: from cells to ecosystems. Oceanography 20, 89–100.

Catalá, T.S., Ortega-Retuerta, E., Calvo, E., Álvarez, M., Fuentes-Lema, A., Reche, I., Romera-Castillo, C., Marrasé, C., Stedmon, C.A., Nieto-Cid, M., Álvarez-Salgado, X.A., Fuentes-Lema, A., Romera-Castillo, C., Nieto-Cid, M., Ortega-Retuerta, E., Calvo, E., Álvarez, M., Marrasé, C., Stedmon, C.A., Álvarez-Salgado, X.A., 2015. Turnover time of fluorescent dissolved organic matter in the dark global ocean. Nat. Commun. 6, 5986. https://doi.org/10.1038/ncomms6986.

Chaidez, V., Dreano, D., Agusti, S., Duarte, C.M., Hoteit, I., 2017. Decadal trends in Red Sea maximum surface temperature. Sci. Rep. 7, 8144. https://doi.org/10.1038/s41598-017-08146-z.

Church, M.J., Ducklow, H.W., Karl, D.M., 2004. Light dependence of [3H] leucine incorporation in the oligotrophic North Pacific Ocean. Appl. Environ. Microbiol. 70, 4079–4087.

Coble, P.G., 2007. Marine optical biogeochemistry: the chemistry of ocean color. Chem. Rev. 107, 402–418.

Coble, P.G., Lead, J., Baker, A., Reynolds, D.M., Spencer, R.G.M., 2014. Aquatic Organic Matter Fluorescence. Cambridge University Press.

Cotner, J.B., Biddanda, B.A., 2002. Small players, large role: microbial influence on biogeochemical processes in pelagic aquatic ecosystems. Ecosystems 5, 105–121. https://doi.org/10.1007/s10021-001-0059-3.

Del Giorgio, P.A., Gasol, J.M., 2008. Physiological structure and single-cell activity in marine bacterioplankton. Microb. Ecol. Ocean. 2, 243–285.

Dinsdale, E.A., Rohwer, F., 2011. Fish or germs? Microbial dynamics associated with changing trophic structures on coral reefs. Coral Reefs: An Ecosystem in Transition. Springer, pp. 231–240.

Done, T.J., 1992. Phase shifts in coral reef communities and their ecological significance. Hydrobiologia 247, 121–132. https://doi.org/10.1007/BF00008211.

Done, T.T.J., Ogden, J.J.C., Wiebe, W., Rosen, B., 1996. Biodiversity and ecosystem function of coral reefs. Global Biodiversity Assessment. John Wiley & Sons, pp. 393–429.

Ezzat, L., Maguer, J.-F., Grover, R., Ferrier-Pagès, C., 2016. Limited phosphorus availability is the Achilles heel of tropical reef corals in a warming ocean. Sci. Rep. 6, 31768.

Ferrera, I., Sánchez, O., Kolářová, E., Koblížek, M., Gasol, J.M., 2017. Light enhances the growth rates of natural populations of aerobic anoxygenic phototrophic bacteria. ISME J 11, 2391–2393.

Gasol, J.M., Moran, X.A.G., 2015. Flow cytometric determination of microbial abundances and its use to obtain indices of community structure and relative activity. Hydrocarb. Lipid Microbiol. Protoc. - Springer Protoc. Handbooks, pp. 1–29 https://doi.org/10.1007/8623.

del Giorgio, P.A., Cole, J.J., 1998. Bacterial growth efficiency in natural aquatic systems. Annu. Rev. Ecol. Syst. 29, 503–541. https://doi.org/10.1146/annurev.ecolsys.29.1.503.

Grégori, G., Citterio, S., Ghiani, A., Labra, M., Sgorbati, S., Brown, S., Denis, M., 2001. Resolution of viable and membrane-compromised Bacteria in freshwater and marine waters based on analytical flow Cytometry and nucleic acid double staining. Appl. Environ. Microbiol. 67, 4662–4670. https://doi.org/10.1128/AEM.67.10.4662-4670.2001.

Gundersen, K., Heldal, M., Norland, S., Purdie, D.A.A., Knap, A.H.H., 2002. Elemental C, N, and P cell content of individual bacteria collected at the Bermuda Atlantic Time-Series Study (BATS) site. Limnol. Oceanogr. 47, 1525–1530. https://doi.org/10.4319/lo.2002.47.5.1525.

Haas, A.F., Wild, C., 2010. Composition analysis of organic matter released by cosmopolitan coral reef-associated green algae. Aquat. Biol. 10, 131–138. https://doi.org/10.3354/ab00271.

Haas, A.F., Naumann, M.S., Struck, U., Mayr, C., el-Zibdah, M., Wild, C., 2010. Organic matter release by coral reef associated benthic algae in the Northern Red Sea. J. Exp. Mar. Bio. Ecol. 389, 53–60. https://doi.org/10.1016/j.jembe.2010.03.018.

Haas, A.F., Nelson, C.E., Kelly, L.W., Carlson, C.A., Rohwer, F., Leichter, J.J., Wyatt, A., Smith, J.E., 2011. Effects of coral reef benthic primary producers on dissolved organic carbon and microbial activity. PLoS One 6. https://doi.org/10.1371/journal.pone.0027973.

Haas, A.F., Nelson, C.E., Rohwer, F., Wegley-Kelly, L., Quistad, S.D., Carlson, C.A., Leichter, J.J., Hatay, M., Smith, J.E., 2013. Influence of coral and algal exudates on microbially mediated reef metabolism. PeerJ 1, e108. https://doi.org/10.7717/peerj.108.

Haas, A.F., Fairoz, M.F.M., Kelly, L.W., Nelson, C.E., Dinsdale, E.A., Edwards, R.A., Giles, S., Hatay, M., Hisakawa, N., Knowles, B., Lim, Y.W., Maughan, H., Pantos, O., Roach, T.N.F., Sanchez, S.E., Silveira, C.B., Sandin, S., Smith, J.E., Rohwer, F., 2016. Global microbialization of coral reefs. Nat. Microbiol. 1, 1–7. https://doi.org/10.1038/nmicrobiol.2016.42.

Heron, S.F., Maynard, J.A., Van Hooidonk, R., Eakin, C.M., 2016. Warming trends and bleaching stress of the world's coral reefs 1985–2012. Sci. Rep. 6, 38402.

Huete-Stauffer, T.M., Arandia-Gorostidi, N., Díaz-Pérez, L., Morán, X.A.G., 2015. Temperature dependences of growth rates and carrying capacities of marine bacteria depart from metabolic theoretical predictions. FEMS Microbiol. Ecol. 91, 1–10. https://doi.org/10.1093/femsec/fiv111.

Huete-Stauffer, T.M., Arandia-Gorostidi, N., González-Benítez, N., Díaz-Pérez, L., Calvo-Díaz, A., Morán, X.A.G., 2017. Large plankton enhance heterotrophy under experimental warming in a temperate coastal ecosystem. Ecosystems, 1–16 https://doi.org/10.1007/s10021-017-0208-y.

Hughes, T.P., Kerry, J.T., Baird, A.H., Connolly, S.R., Dietzel, A., Eakin, C.M., Heron, S.F., Hoey, A.S., Hoogenboom, M.O., Liu, G., McWilliam, M.J., Pears, R.J., Pratchett, M.S., Skirving, W.J., Stella, J.S., Torda, G., 2018. Global warming transforms coral reef assemblages. Nature, 1–5 https://doi.org/10.1038/s41586-018-0041-2.

Huguet, A., Vacher, L., Relexans, S., Saubusse, S., Froidefond, J.M., Parlanti, E., 2009. Properties of fluorescent dissolved organic matter in the Gironde estuary. Org. Geochem. 40, 706–719. https://doi.org/10.1016/j.orggeochem.2009.03.002.

Kirchman, D.L., Morán, X.A.G., Ducklow, H., 2009. Microbial growth in the polar oceans - role of temperature and potential impact of climate change. Nat. Rev. Microbiol. 7, 451–459. https://doi.org/10.1038/nrmicro2115.

Lemée, R., Rochelle-Newall, E., Van Wambeke, F., Pizay, M.-D., Rinaldi, P., Gattuso, J.-P., 2002. Seasonal variation of bacterial production, respiration and growth efficiency in the open NW Mediterranean Sea. Aquat. Microb. Ecol. 29, 227–237.

Lønborg, C., Cuevas, L.A., Reinthaler, T., Herndl, G.J., Gasol, J.M., Morán, X.A.G., Bates, N.R., Álvarez-Salgado, X.A., 2016a. Depth dependent relationships between temperature and ocean heterotrophic prokaryotic production. Front. Mar. Sci. 3, 90.

Lønborg, C., Nieto-Cid, M., Hernando-Morales, V., Hernández-Ruiz, M., Teira, E., Álvarez-Salgado, X.A., 2016b. Photochemical alteration of dissolved organic matter and the subsequent effects on bacterial carbon cycling and diversity. FEMS Microbiol. Ecol. 92, 1–14. https://doi.org/10.1093/femsec/fiw048.

Lønborg, C., Álvarez–Salgado, X.A., Duggan, S., Carreira, C., 2018. Organic matter bioavailability in tropical coastal waters: the Great Barrier Reef. Limnol. Oceanogr. 63, 1015–1035.

Lønborg, C., Baltar, F., Carreira, C., Morán, X.A.G., 2019. Dissolved organic carbon source influences tropical coastal heterotrophic bacterioplankton response to experimental warming. Front. Microbiol. 10, 2807.

Marie, D., Partensky, F., Jacquet, S., Vaulot, D., 1997. Enumeration and cell cycle analysis of natural populations of marine picoplankton by flow cytometry using the nucleic acid stain SYBR Green I. Appl. Environ. Microbiol. 63, 186–193.

McDole Somera, T., Bailey, B., Barott, K., Grasis, J., Hatay, M., Hilton, B.J., Hisakawa, N., Nosrat, B., Nulton, J., Silveira, C.B., 2016. Energetic differences between bacterioplankton trophic groups and coral reef resistance. Proc. R. Soc. B Biol. Sci. 283, 20160467. https://doi.org/10.1098/rspb.2016.0467.

McKnight, D.M., Boyer, E.W., Westerhoff, P.K., Doran, P.T., Kulbe, T., Andersen, D.T., 2001. Spectrofluorometric characterization of dissolved organic matter for indication of precursor organic material and aromaticity. Limnol. Oceanogr. 46, 38–48.

Michelou, V.K., Cottrell, M.T., Kirchman, D.L., 2007. Light-stimulated bacterial production and amino acid assimilation by cyanobacteria and other microbes in the North Atlantic Ocean. Appl. Environ. Microbiol. 73, 5539–5546.

Monroe, A.A., Ziegler, M., Roik, A., Röthig, T., Hardenstine, R.S., Emms, M.A., Jensen, T., Voolstra, C.R., Berumen, M.L., 2018. In situ observations of coral bleaching in the central Saudi Arabian Red Sea during the 2015/2016 global coral bleaching event. PLoS One 13, e0195814.

Morán, X.A.G., Estrada, M., Gasol, J.M., Pedrós-Alió, C., 2002. Dissolved primary production and the strength of phytoplankton-bacterioplankton coupling in contrasting marine regions. Microb. Ecol. 44, 217–223. https://doi.org/10.1007/s00248-002-1026-z.

Morán, X.A.G., Baltar, F., Carreira, C., Lønborg, C., 2020. Responses of physiological groups of tropical heterotrophic bacteria to temperature and DOM additions: food matters more than warming. Environ. Microbiol. 00. https://doi.org/10.1111/1462-2920.15007.

Morrow, K.M., Paul, V.J., Liles, M.R., Chadwick, N.E., 2011. Allelochemicals produced by Caribbean macroalgae and cyanobacteria have species-specific effects on reef coral microorganisms. Coral Reefs 30, 309–320. https://doi.org/10.1007/s00338-011-0747-1.

Mueller, B., Van Der Zande, R.M., Van Leent, P.J.M., Meesters, E.H., Vermeij, M.J.A., Van Duyl, F.C., 2014. Effect of light availability on dissolved organic carbon release by Caribbean reef algae and corals. Bull. Mar. Sci. 90, 875–893.

Murphy, K.R., Butler, K.D., Spencer, R.G.M., Stedmon, C.A., Boehme, J.R., Aiken, G.R., 2010. Measurement of dissolved organic matter fluorescence in aquatic environments: an interlaboratory comparison. Environ. Sci. Technol. 44, 9405–9412.

Murphy, K.R., Stedmon, C.A., Graeber, D., Bro, R., 2013. Fluorescence spectroscopy and multi-way techniques. PARAFAC. Anal. Methods 5, 6557–6566.

Naumann, M.S., Haas, A., Struck, U., Mayr, C., el-Zibdah, M., Wild, C., 2010. Organic matter release by dominant hermatypic corals of the Northern Red Sea. Coral Reefs 29, 649–659. https://doi.org/10.1007/s00338-010-0612-7.

Nelson, C.E., Alldredge, A.L., McCliment, E.A., Amaral-Zettler, L.A., Carlson, C.A., 2011. Depleted dissolved organic carbon and distinct bacterial communities in the water column of a rapid-flushing coral reef ecosystem. ISME J 5, 1374–1387. https://doi.org/10.1038/ismej.2011.12.

Nelson, C.E., Goldberg, S.J., Wegley Kelly, L., Haas, A.F., Smith, J.E., Rohwer, F., Carlson, C.A., 2013. Coral and macroalgal exudates vary in neutral sugar composition and differentially enrich reef bacterioplankton lineages. ISME J 7, 962–979. https://doi.org/10.1038/ismej.2012.161.

Ohno, T., 2002. Fluorescence inner-filtering correction for determining the humification index of dissolved organic matter. Environ. Sci. Technol. 36, 742–746.

Pratchett, M.S., Bellwood, D.R., Ceccarelli, D., McCook, L., Hoegh-Guldberg, O., Moltschaniwskyj, N., Willis, B., Rodrigues, M.J., Hughes, T.P., Steneck, R.S., 2007. Phase shifts, herbivory, and the resilience of coral reefs to climate change. Curr. Biol. 17, 360–365. https://doi.org/10.1016/j.cub.2006.12.049.

Quinlan, Z.A., Remple, K., Fox, M.D., Silbiger, N.J., Oliver, T.A., Putnam, H.M., Wegley Kelly, L., Carlson, C.A., Donahue, M.J., Nelson, C.E., 2018. Fluorescent organic exudates of corals and algae in tropical reefs are compositionally distinct and increase with nutrient enrichment. Limnol. Oceanogr. Lett. 723868. https://doi.org/10.1002/lol2.10074.

Rix, L., de Goeij, J.M., van Oevelen, D., Struck, U., Al-Horani, F.A., Wild, C., Naumann, M.S., 2017. Differential recycling of coral and algal dissolved organic matter via the sponge loop. Funct. Ecol. 31, 778–789. https://doi.org/10.1111/1365-2435.12758.

Rix, L., De Goeij, J.M., Van Oevelen, D., Struck, U., Al-Horani, F.A., Wild, C., Naumann, M.S., 2018. Reef sponges facilitate the transfer of coral-derived organic matter to their associated fauna via the sponge loop. Mar. Ecol. Prog. Ser. 589, 85–96. https://doi.org/10.3354/meps12443.

Robinson, C., 2008. Heterotrophic bacterial respiration. Microb. Ecol. Ocean. 299–334.

Roth, F., 2019. Consequences of Coral-Algal Phase Shifts for Tropical Reef Ecosystem Functioning N3 - 10.25781/KAUST-K6KP2.

Roth, F., Wild, C., Carvalho, S., Rädecker, N., Voolstra, C.R., Kürten, B., Anlauf, H., El-Khaled, Y.C., Carolan, R., Jones, B.H., 2019. An in situ approach for measuring biogeochemical fluxes in structurally complex benthic communities. Methods Ecol. Evol. 10 (5), 712–725.

Ruiz-González, C., Galí, M., Lefort, T., Cardelús, C., Simó, R., Gasol, J.M., 2012. Annual variability in light modulation of bacterial heterotrophic activity in surface northwestern Mediterranean waters. Limnol. Oceanogr. 57, 1376–1388.

Ruiz-González, C., Simó, R., Sommaruga, R., Gasol, J.M., 2013. Away from darkness: a review on the effects of solar radiation on heterotrophic bacterioplankton activity. Front. Microbiol. 4, 131.

Sawall, Y., Al-Sofyani, A., Hohn, S., Banguera-Hinestroza, E., Voolstra, C.R., Wahl, M., 2015. Extensive phenotypic plasticity of a Red Sea coral over a strong latitudinal temperature gradient suggests limited acclimatization potential to warming. Sci. Rep. 5, 8940.

Sherr, B.F., Del Giorgio, P., Sherr, E.B., 1999. Estimating abundance and single-cell characteristics of respiring bacteria via the redox dye CTC. Aquat. Microb. Ecol. 18, 117–131. https://doi.org/10.3354/ame018117.

Sierra, C.A., 2012. Temperature sensitivity of organic matter decomposition in the Arrhenius equation: some theoretical considerations. Biogeochemistry 108, 1–15.

Silva, L., Calleja, M.L., Huete-Stauffer, T.M., Ivetic, S., Ansari, M.I., Viegas, M., Morán, X.A.G., 2019. Low abundances but high growth rates of coastal heterotrophic bacteria in the Red Sea. Front. Microbiol. 9, 1–15. https://doi.org/10.3389/fmicb.2018.03244.

Silveira, C.B., Silva-Lima, A.W., Francini-Filho, R.B., Marques, J.S.M., Almeida, M.G., Thompson, C.C., Rezende, C.E., Paranhos, R., Moura, R.L., Salomon, P.S., Thompson, F.L., 2015. Microbial and sponge loops modify fish production in phase-shifting coral reefs. Environ. Microbiol. 17, 3832–3846. https://doi.org/10.1111/1462-2920.12851.

Silveira, C.B., Luque, A., Roach, T.N., Villela, H., Barno, A., Green, K., Reyes, B., Rubio-Portillo, E., Le, T., Mead, S., Hatay, M., Vermeij, M.J., Takeshita, Y., Haas, A., Bailey, B., Rohwer, F., 2019. Biophysical and physiological processes causing oxygen loss from coral reefs. Elife 8, 1–24. https://doi.org/10.7554/eLife.49114.

Smith, E.M., 1998. Coherence of microbial respiration rate and cell-specific bacterial activity in a coastal planktonic community. Aquat. Microb. Ecol. 16, 27–35. https://doi.org/10.3354/ame016027.

Smith, J.E., Shaw, M., Edwards, R.A., Obura, D., Pantos, O., Sala, E., Sandin, S.A., Smriga, S., Hatay, M., Rohwer, F.L., 2006. Indirect effects of algae on coral: algae-mediated, microbe-induced coral mortality. Ecol. Lett. 9, 835–845.

Spalding, M.D., Brown, B.E., 2015. Warm-water coral reefs and climate change. Science (80-.) 350, 769–771.

Stedmon, C.A., Bro, R., 2008. Characterizing dissolved organic matter fluorescence with parallel factor analysis: a tutorial. Limnol. Oceanogr. Methods 6, 572–579.

Stedmon, C.A., Markager, S., Bro, R., 2003. Tracing dissolved organic matter in aquatic environments using a new approach to fluorescence spectroscopy. Mar. Chem. 82, 239–254.

Vrede, K., Heldal, M., Norland, S., Bratbak, G., 2002. Elemental composition (C, N, P) and cell volume of exponentially growing and nutrient-limited bacterioplankton. Appl. Environ. Microbiol. 68, 2965–2971.

Wild, C., Niggl, W., Naumann, M.S., Haas, A.F., 2010. Organic matter release by Red Sea coral reef organisms-potential effects on microbial activity and in situ O2 availability. Mar. Ecol. Prog. Ser. 411, 61–71. https://doi.org/10.3354/meps08653.

Wild, C., Hoegh-Guldberg, O., Naumann, M.S., Colombo-Pallotta, M.F., Ateweberhan, M., Fitt, W.K., Iglesias-Prieto, R., Palmer, C., Bythell, J.C., Ortiz, J.C., Loya, Y., Van Woesik, R., 2011. Climate change impedes scleractinian corals as primary reef ecosystem engineers. Mar. Freshw. Res. 62, 205–215. https://doi.org/10.1071/MF10254.